EUROFUSION WPS2-CP(16) 15283

J. Geiger et al.

Plasma Effects in Full-Field MHD-Equilibrium Calculations for W7-X

Preprint of Paper to be submitted for publication in
Proceedings of 26th IAEA Fusion Energy Conference

This work has been carried out within the framework of the EUROfusion Consortium and has received funding from the Euratom research and training programme 2014-2018 under grant agreement No 633053. The views and opinions expressed herein do not necessarily reflect those of the European Commission.

Plasma Effects in Full-Field MHD-Equilibrium Calculations for W7-X

J. Geiger[1], C.D. Beidler[1], Y. Feng[1], P. Helander[1], H. Hölbe[1], H. Maassberg[1], Y. Suzuki[2,3], and Y. Turkin[1]

[1] Max-Planck-Institute for Plasma Physics, D-17491 Greifswald, Germany
[2] National Institute for Fusion Science, Oroshi-cho 322-6, 509-5292, Japan
[3] SOKENDAI, Grad. Universities for Advanced Studies, Oroshi-cho 322-6, 509-5292, Japan

E-mail contact of main author: joachim.geiger@ipp.mpg.de

Abstract. Wendelstein 7-X aims at quasi-steady-state operation to demonstrate the reactor-viability of stellarators optimized with respect to MHD-equilibrium and -stability, low neoclassical transport, small bootstrap current and good fast-particle confinement. For particle and energy exhaust an island-divertor is foreseen utilizing naturally occurring boundary islands connected with low-order rational values of the rotational transform at the plasma boundary. The island separatrix bounds the plasma, and the strike lines of the island fans determine the heat load distribution on the divertor structures. Although being optimized to display a small impact of plasma currents on the magnetic geometry, these effects still exist in W7-X and change the plasma shape and the boundary islands' width and location. The configurations considered here are expected to have a bootstrap current which is small enough (according to transport simulations) to allow high-performance, quasi-steady-state operation compatible with the island divertor without additional boundary-iota control schemes, e.g. ECCD. Based on the VMEC-EXTENDER code a special combination of the calculated magnetic fields is used to investigate effects of plasma-β and net-toroidal currents on the boundary islands. Connection length calculations as well as calculations of the footprints of the field lines on the divertor parts show the different shadowing effects of the divertor geometry on the boundary islands as well as their radial dislocation in case of different net-currents. Comparitive calculations using the HINT-code have been started and show general agreement but also systematic differences that need further investigations.

1. Introduction

Wendelstein 7-X aims at quasi-steady-state operation to demonstrate the reactor-viability of stellarators optimized with respect to MHD-equilibrium and -stability, low neoclassical transport, small bootstrap current (I_{bc}) and good fast-particle confinement [1]. To reach this goal a 10MW cw-ECRH system (140GHz) [2] has been installed to allow high-performance plasmas to be achieved, and the island divertor concept has been chosen for particle and energy exhaust [3, 4]. The island divertor utilizes the naturally occurring islands connected with the appearance of low-order rational values of the rotational transform ι at the plasma boundary. The island separatrix thus bounds the plasma, and the strike lines of the island fans guide the particle and energy fluxes, thus determining the heat load distribution on the divertor structures.

Although the configuration of W7-X has been optimized to minimize the impact of plasma currents on the magnetic geometry, such effects still exist and change the plasma shape and the boundary islands' width and location. The optimization that was performed in the design of W7-X is a point-optimization, where in a single configuration all optimization targets were combined in a reasonable compromise. Within the actual coil system, this configuration is realized in the so-called high-mirror reference configuration. Moving away from the optimization point in the space of magnetic configurations by adjusting the currents in the various magnetic-field coils, one can improve some properties of the plasma at the expense of others. The plasma-β effects that exist despite the optimization are known, for example, to lead to an increase in the island widths with growing plasma-β [5, 3, 6] while X- and O-point locations move poloidally, consistently with the effect of the Shafranov-shift. Net toroidal currents are known to shift the island-generating resonances radially, which, depending on the amount of plasma current, can lead to undesired deviations from proper island divertor operation, e.g. by

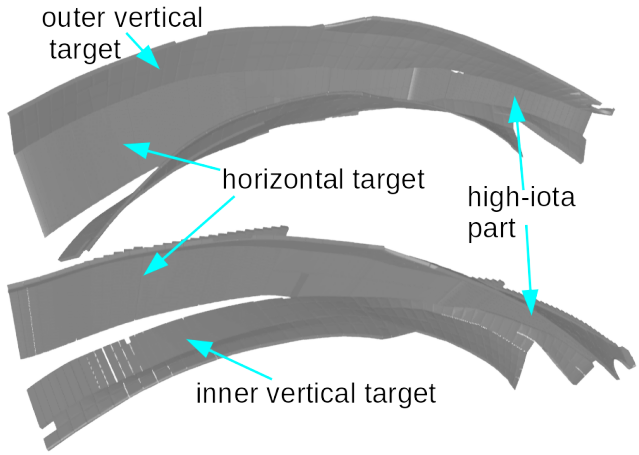

Fig. 1: Two views into a divertor module. In each of the 5 periods a stellarator-symmetric combination of an upper and lower divertor module, i.e. 10 in total, is installed for particle and energy exhaust. Between horizontal and inner vertical target is the pumping gap. The paper uses the lower view.

moving island structures away from the divertor plates, resulting in a limiter magnetic configuration [7] or in heat loads misdirected to critical components [8]. Fig. 1 shows the divertor geometry from two slightly different views.

In order to investigate the effects of plasma-β and of net-toroidal currents on the width and location of boundary islands and the impact on the interaction of the plasma with the divertor, magnetic fields in the entire plasma vessel are needed and not only inside the plasma. Other applications relying on such fields are NBI-deposition calculations accounting for re-entering ions or transport simulations of the scrape-off-layer with codes like EMC3-/EIRENE. The VMEC-EXTENDER [7] approach offers a straightforward way of generating such fields with the advantage of a flexible handling of plasma profiles via VMEC [9]. The approach, however, does not result in a fully self-consistent equilibrium field, but approximates this very well outside the VMEC-domain. Nevertheless, in order to explore the limitations of the approach, the 3D MHD-equilibrium code HINT [10,11] is used to compare the results to. HINT's numerical scheme does not rely on the existence of flux surfaces as VMEC does and thus allows the self-consistent treatment of islands and stochastic regions and calculates the field self-consistently in a much larger region including the vessel volume.

The paper first introduces the VMEC/EXTENDER-method, and then magnetic configurations and experimental scenarios are used to produce results in terms of Poincaré-plots, connection length (L_C) calculations and footprints on the divertors. Finally, a comparison of some cases with calculations based on the HINT-code are shown and similarities and differences are discussed.

2. Method

The approach for full-field calculations used here is based on the VMEC-EXTENDER code combination [6, 9]. VMEC is the work-horse for MHD-equilibrium calculations but has the drawback that its mathematical treatment requires the existence of nested flux surfaces and thus cannot treat islands or stochastic regions. It also calculates the equilibrium fields only up to the last flux surface that it assumes to exist. Fields outside this domain are not available but interact with the equilibrium via the boundary condition for the equilibrium calculation in the so-called free-boundary mode. However, fields which extend beyond the VMEC-calculation domain are needed for example in NBI deposition calculations accounting for those fast ions that leave the plasma but re-enter and contribute to the heating, or in transport simulations of the scrape-off-layer with codes like EMC3/EIRENE [12], which are used for investigating divertor operation scenarios for W7-X. The fields outside the VMEC-domain can be calculated using the EXTENDER code, which applies the virtual casing principle for this purpose. A full field can then be generated by combining the VMEC-solution inside the VMEC-domain with

the field outside obtained by summing up the plasma response from EXTENDER and the vacuum field via Biot-Savart from external coils. Unfortunately, such a field combination violates the condition $\nabla\cdot\mathbf{B}=0$ at the interface of the two field combinations by an amount that is too large in general for EMC3-calculations. A way around this problem is possible by instead exploiting the fact that the virtual casing principle allows the vacuum field seen by VMEC inside the VMEC-domain to be calculated. Subtracting this field from the full VMEC-field provides the plasma-generated fields inside the VMEC-domain. Thus, the plasma-generated fields are now available everywhere and can be combined with the Biot-Savart field to a full-field solution which still violates $\nabla\cdot\mathbf{B}=0$ at the "plasma boundary" but to a degree that EMC3 can tolerate. Note that these fields are no longer exact MHD-equilibrium fields, as the connection between the existence of flux surfaces and the field is broken. This becomes obvious since in these fields islands can be observed in the VMEC-domain, and if a low-order rational generates a separatrix-producing boundary island chain, this separatrix or stochastic fields can penetrate into the VMEC-domain. Hanson has given an explanation to this puzzle by pointing out that there can be non-zero surface currents on the VMEC-boundary, which can theoretically explain the difference in the two field combinations [13, 14]. To some extent, the discrepancy may be a signal that the VMEC-domain has been chosen too large and needs to be shrunk. However, even with an adjusted size of the VMEC-calculations, the second way of combining the fields as described above still has a smaller violation of $\nabla\cdot\mathbf{B}=0$ and is therefore preferred for EMC3-calculations.

To investigate the resulting fields, we use field-line tracing, and to simulate SOL-transport a diffusion process is added to the field-line tracing, i.e. field-line diffusion. To study the interaction with the divertor geometry (see Fig. 1) the field lines are started inside the last closed flux surface, but close to it, and are traced until they intersect an in-vessel component and then recorded to belong to the corresponding component. In this way, a first estimate of heat loads on different in-vessel components can be derived.

The sequence of codes, i.e. VMEC and EXTENDER, and the field-line tracing/diffusion codes using the resulting fields are available at IPP as webservices [15] and the chain is connected by python scripts and python modules to convert the fields to different formats.

3. Magnetic Configurations

The magnetic configurations considered here resulted from a conservative approach to quasi-steady-state divertor operation in high-performance (large $n\mathrm{T}\tau$), high-density scenarios within the configuration space of W7-X (see [16] for details on the scenarios) by aiming at negligible I_{bc} for configurations with the three low-order rational boundary-ι values for a proper divertor magnetic topology, namely ι_b= 5/6, 5/5 and 5/4, usually denoted as low-ι, standard-ι and high-ι, respectively. The investigation applied an iteration loop combining VMEC-calculations, evaluation of neoclassical transport coefficients with DKES [17] and transport simulations using the NTSS-code [18] until a negligible I_{bc} had been achieved in a consistent combination of equilibrium, transport coefficients and neoclassical transport simulations. The focus in [16] was on core confinement and equilibrium, and a fine-tuning of the magnetic configuration for good divertor compatibility was not attempted. The main result was that the toroidal mirror field, as measured by the Fourier coefficient B_{01} in Boozer coordinates normalized to B_{00}, i.e. $b_{01}=B_{01}/B_{00}$, varies strongly with ι to achieve a negligible I_{bc} at different ι-values. In detail, the high-ι case was acceptable with b_{01}=4%, the standard-ι case required b_{01}=11%, while the low-ι case demanded b_{01}=24%, which is comparatively large considering that the reference configurations reach up to values of $b_{01}\approx$10%. Additionally, variations of the heating scenarios, i.e.

on-axis vs off-axis ECRH, could result in a variation of I_{bc} of the order of 5 to 10kA.

4. VMEC/EXTENDER-results

First, only changes of the plasma boundary due the effect of the plasma-β are considered by a β-scan (p~1-s, s = norm. tor. flux) in the standard-ι configuration with mr≈11%. Fig.2 compares a low and a medium β-calculation overlaying the Poincaré-plot with the color-coded values of L_C calculated for the φ=0° plane (scale: $\log_{10}(L_C+1)$, in m: red=10^3m). The boundary island width increases with increasing β, an effect already known from [5, 6]. The L_C-colors clearly show the shadowing effects of the divertor components. Note that with increasing β, the island o-points are shadowed less. The β-effect can be explored also by studying the footprints of the field lines on the target as shown in Fig.3 (a and b) for the same two fields revealing other aspects. In this case, the strike-line on the vertical target (see Fig.1 for comparison) is the most prominent at low-β but extends toroidally as β increases. The small footprint on the horizontal target near the pumping gap increases its toroidal extension also with β. On the horizontal target a new footprint is seen for the case with <β>=3%. This footprint emerges when <β> is increased above 2% while for smaller β-values this footprint is barely visible. If field-line diffusion is considered as an additional effect to mimic SOL-transport, then the footprints get spread out. This will reduce the local heat loads but at the same time may also load other parts of the divertor. Note that in the case shown in Fig.3 c) and d) the increase in β reduces the spreading of the footprint on the vertical target. The effect of a varying I_{bc} (different profiles or heating scenarios) is

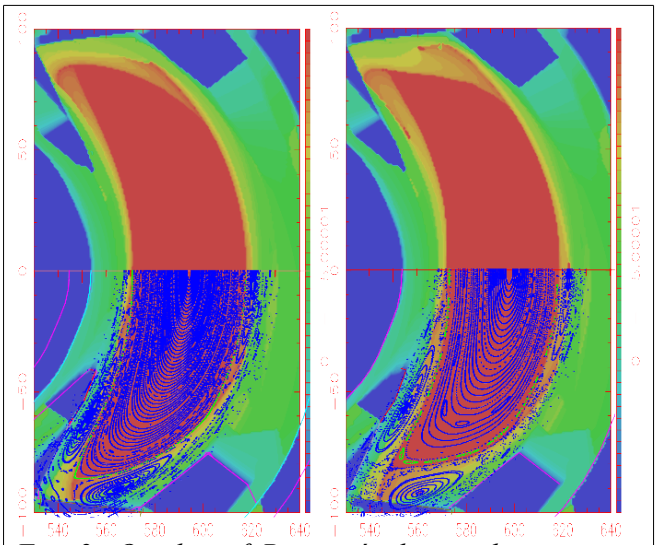

Fig. 2: Overlay of Poincaré plots and connection lengths calculated for the φ=0°-cross section. Configuration with mr=11% at ι=1 for different β-values of the VMEC-calculation. Left: <β>=1%; right: <β>=3%.

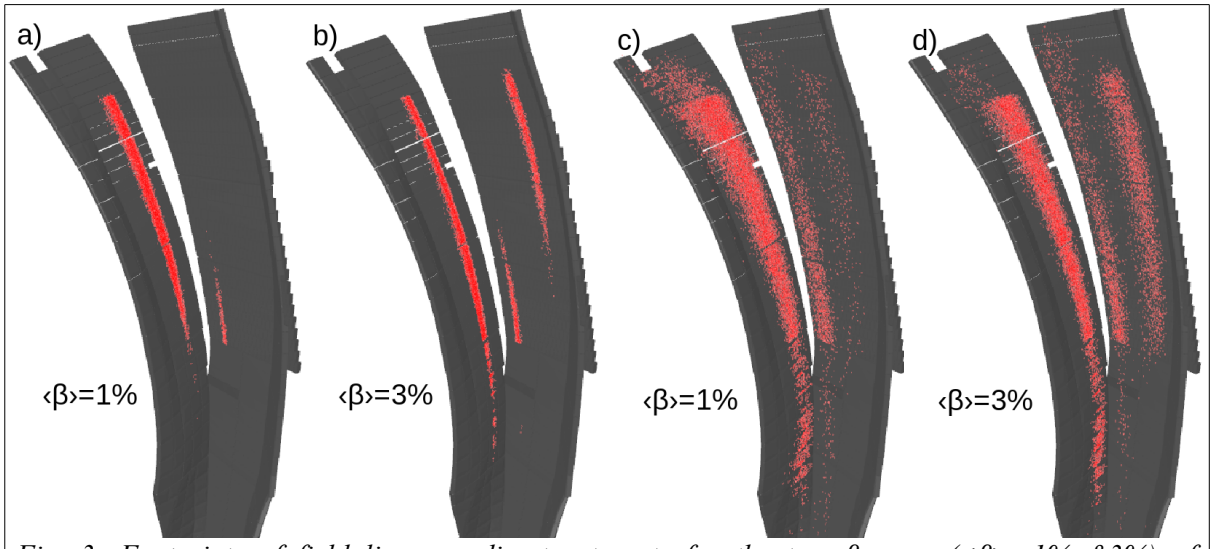

Fig. 3: Footprints of field lines on divertor targets for the two β-cases (<β>=1% &3%) of Fig.1with negligible (a and b) and with considerable (c and d) field-line diffusion. The two diffusion cases have $D_\perp/D_\parallel=5\cdot10^{-7}$ and ca $1\cdot10^{-5}$.

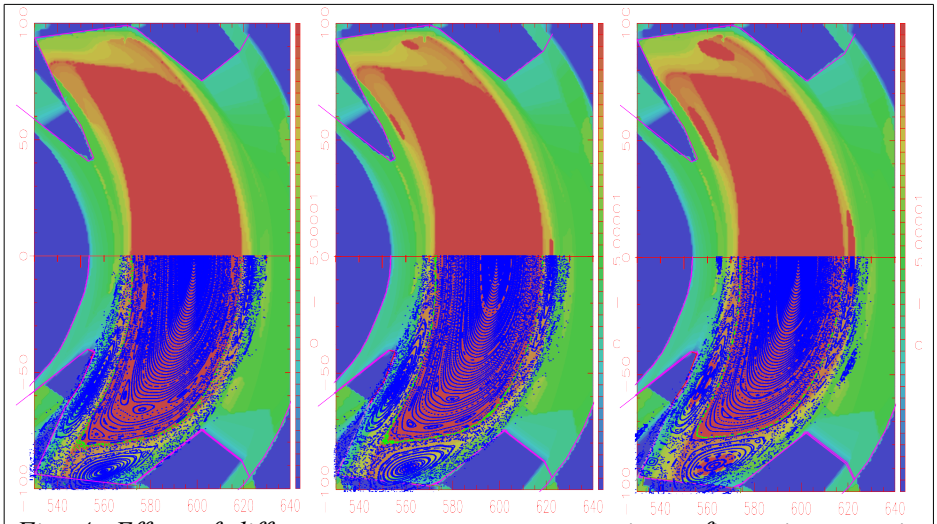

Fig. 4: Effect of different net-currents on magnetic configuration seen in Poincaré-plots (only lower part shown) and on shadowing by divertor components visible by colour-coded connection length. From left to right: Ipl=-3.43kA, 3.43kA, 10.29kA.

investigated by a scan of the net-current. Fig.4 shows the color-coded L_C with overlayed Poincare plots showing the magnetic topology. The middle case is the one expected from neoclassical transport simulations while for the left and the right case the net-current was scaled by -1 and +3, respectively, thus resulting in a variation of about ±7kA. Two effects are clearly seen, first the radial movement of the resonance position, i.e. the o- and x-point locations, and second, due to this movement the o-point is shadowed less when I_{bc} becomes more positive. This might have an impact on the plasma-divertor interaction and the neutral-shielding since cold plasma might be confined in this non-shadowed region around the o-point of the island. Fig.5 reveals the effect of the radial dislocation of the boundary island in view of the footprints on the divertor. The distance between the two strike lines on the horizontal target decreases as the net-current becomes more positive, i.e. as the boundary island moves radially away from the target plates. On the vertical target, the toroidal extent of the strike line becomes shorter and broadens. The latter might reflect that the *outer* (away from the plasma) island separatrix and the vertical divertor plate are closely aligned.

Fig. 5: Effect of different net-currents on magnetic configuration visible by footprints of field lines on vertical and horizontal targets. As previously from left to right: Ipl=-3.43kA, 3.43kA, 10.29kA.

The high-ι configuration differs from the standard-ι and low-ι configuration in that its boundary islands start with a considerable, stochastic region between the remaining good flux surfaces around the o-points of the island and the separatrix of the main plasma. This is a property of the reference high-ι configuration as well as of the configuration in [16]. This can be seen in Fig.6 (left

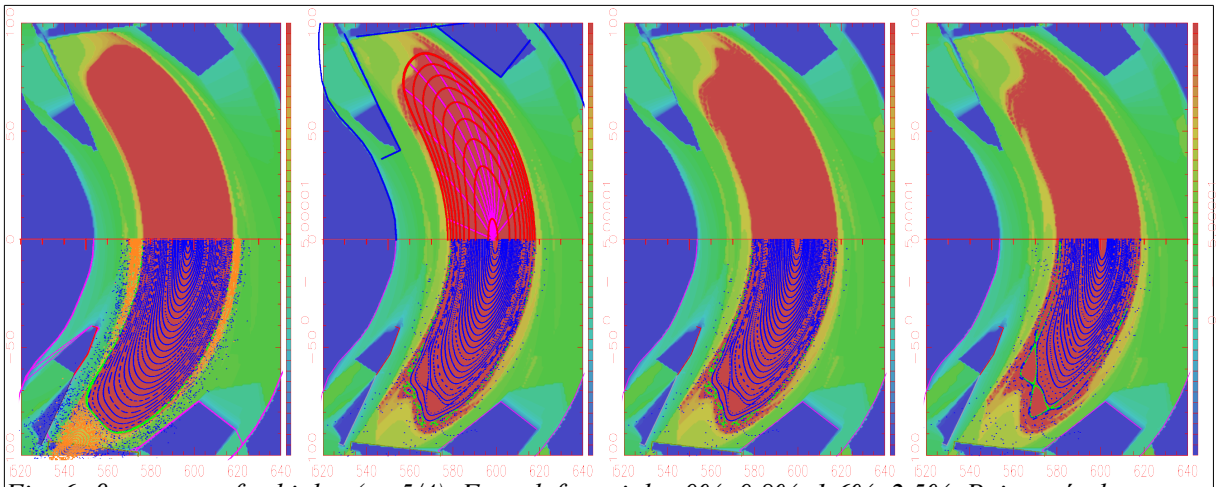

Fig. 6: β-sequence for high-ι (ι_b=5/4). From left to right: 0%, 0.8%, 1.6%, 2.5%. Poincaré-plot put on top of connection length plots (same colour-code as before). In the vacuum case the boundary island are shown, too.

most picture). Fig.6 also shows the increasing degradation of the magnetic configuration as β is increased. Strumberger observed this earlier in the first applications [3] of the VMEC/MFBE-code but the volume had to be adapted as the confinement region shrunk. The effect is also seen in HINT calculations [10] for W7-X. The VMEC-calculations underlying the alternative field combination of Fig.6 have all the same volume (a_{eff}≈46.5cm), but show the shrinking of the good flux surface region. An adaption of the size to smaller volume does not significantly change the result as seen in Fig. 7 where the calculation with the volume used in Fig.6 (a_{eff}=46.5cm) for ‹β›=3.3% is compared to a one with a smaller value (a_{eff}=42.5cm). The location of the 10/9 island forming the separatrix is roughly at the location and the structure of the L_C-contours are also very similar. However, the 15/14 island chain has grown considerably in the smaller volume case. The difference in boundary structure and L_C-distribution is non-negligible, if the VMEC-solution is used inside the VMEC-domain instead. In that case an adjustment of the underlying VMEC-calculation is mandatory for a reasonable agreement, as has been done in Strumberger's VMEC/MFBE-results. It seems that the alternative field combination gives at least a reasonable first guess of the plasma size.

5. Comparison with HINT-calculations

The comparison of the fields resulting from VMEC/EXTENDER and HINT is currently preliminary. Nevertheless, the fields from the two approaches show very similar features although there are differences in the details. Fig.8 shows a comparison of the Poincare-plots of the standard-iota case. The magnetic configuration and the pressure profile are the same as in Fig.4 & 5 but with vanishing net-current density. The β-value is about 3%. The flux surface shape is reproduced quite well, although there is a mismatch of the magnetic axis position (the HINT-result shows a stronger axis-shift), the separatrix is cleaner in the

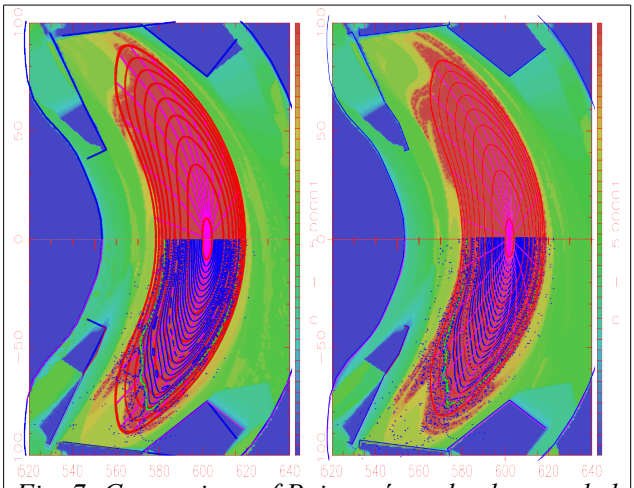

Fig. 7: Comparison of Poincaré- and colour-coded L_C-plots for fields resulting from VMEC-runs with different size for high-ι case with β=3.3%. Left: a_{eff}=46.5cm; Right: 42.5cm. In the right picture, the VMEC flux surfaces are shown, too.

HINT-case and the islands are shifted radially slightly further out. A comparison of the ι-profiles shows that the HINT-profile is about 0.01 lower than the one from VMEC/EXTENDER which explains the radial dislocation of the islands. However, the reason for the ι-mismatch has not yet been identified.

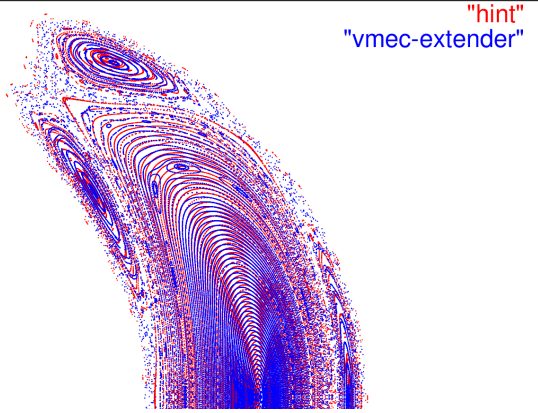

Fig. 8: Overlay of Poincaré plots from HINT-calculation and from VMEC/EXTENDER for the standard-ι_a case in the high-performance phase.

A comparison of the footprint patterns of the field lines on the divertor targets is shown in Fig.9 (left part VMEC/EXTENDER-field, right part HINT-field). Generally they are quite similar and the obvious differences can be explained by the different ι-profiles. Because the islands in the HINT-result are radially displaced further out, the strike-lines on the horizontal target are a bit further apart from each other as in a case of lower ι due to a smaller or more negative net-current (compare to the net-current-scan above, especially the case I_{pl}=-3.43kA). Also the footprints on the vertical inner target show this effect of a lower ι-value.

6. Summary and Conclusions

The VMEC/EXTENDER approach to derive full-fields for investigations of the boundary structures has been implemented and tested for W7-X. The approach allows changes of the magnetic geometry with respect to the divertor due to beta and net-currents to be explored. It seems, that for a first assessment of the boundary topology via the alternative field combination the volume of the underlying VMEC-calculation needs not necessarily have to be entirely consistent with the good surface volume identified by field-line tracing results. This eases a first assessment but allows also to improve the results by adjusting the volume of the VMEC-calculations. Field-line tracing and field-line diffusion are possible and will allow estimating heat load distributions on the divertor. The entire chain from VMEC- and EXTENDER-calculation and the use of field-line tracing and -diffusion codes is available as webservices at IPP and connected with appropriate python-scripts and modules.
Preliminary comparisons to HINT-calculations are promising, showing similar features in the field and in the footprints on the divertor targets, but there are also differences in the results (mismatch of the ι-profile) which need to be clarified. Additional HINT-calculations for the scenarios in [16] have been performed [19] allowing further assessment of the differences.

Fig. 9: Comparison of footprints of field on divertor resulting from VMEC/EXTENDER-calculation (left) and from HINT2 (right).

Acknowledgement

This work has been carried out within the framework of the EUROfusion Consortium and has received funding from the Euratom research and training programme 2014-2018 under grant agreement No 633053. The views and opinions expressed herein do not necessarily reflect those of the European Commission.

References

[1] GRIEGER, G., et al., "Physics optimization of Stellarators", Phys. Fluids B: Plasma Physics **4** (1992) pp 2081-2091
[2] ERCKMANN, V., et al.,"Electron Cyclotron Heating for W7-X: Physics and Technology", Fusion Sci. Technol. **52** (2007) pp 291-312
[3] RENNER, H., et al., "Divertor concept for the W7-X stellarator and mode of operation", Plasma Phys. Control. Fusion **44** (2002) pp 1005
[4] PEACOCK, A., et al., "Status of High Heat Flux Components at W7-X", IEEE Transactions on Plasma Science **42** (2014) pp 524-532
[5] STRUMBERGER, E., "Finite-β magnetic field line tracing for Helias configurations", 1997 Nucl. Fusion **37** (1997) pp 19
[6] DREVLAK, M., et al., "PIES free boundary stellarator equilibria with improved initial conditions", Nucl. Fusion **45** (2005) pp 731
[7] GEIGER, J., et al., "Effects of Net Currents on the Magnetic Configuration of W7-X", Contrib. Plasma Phys. **50** (2010) pp 770
[8] LORE, J., et al., "Design and Analysis of Divertor Scraper Elements for the W7-X Stellarator", IEEE Transactions on Plasma Science **42** (2014) pp 539
[9] HIRSHMAN, S.P., et al., "Three-dimensional free boundary calculations using a spectral green's function method", Comput. Phys. Comm. **43** (1986) pp 143
[10] SUZUKI, Y., et al., "Development and application of HINT2 to helical system plasmas", Nucl. Fusion **46** (2006) pp L19-L24
[11] SUZUKI, Y., et al., "Three-Dimensional Effects on Stochasticity in Non-Axisymmetric Tori", Contrib. Plasma Phys. **50** (2010) pp 576
[12] FENG, Y., et al., "Recent Improvements in the EMC3-Eirene Code", Contrib. Plasma Phys. **54** (2014) pp 426-431
[13] HANSON, J.D., "The virtual-casing principle and Helmholtz's theorem", Plasma Phys. Control. Fusion **57** (2015) 115006
[14] HANSON, J.D., priv. comm. of presentation at APS-DPP, 19.11.2015, Savannah, Georgia
[15] BOZHENKOV, S. et al., "Service oriented architecture for scientific analysis at W7-X. An example of a field line tracer" Fus. Eng. Des. **88** (2013) 2997-3006
[16] GEIGER, J., et al., "Physics in the magnetic configuration space of W7-X", Plasma Phys.Control. Fusion **57** (2015) 014004
[17] VAN RIJ, W. I. and HIRSHMAN, S. P., "Variational bounds for transport coefficients in three-dimensional toroidal plasmas", Phys. Fluids B **1** (1989) pp 563-569
[18] TURKIN, Y., et al., "Neoclassical transport simulations for stellarators", Phys. Plasmas **18** (2011) 022505
[19] SUZUKI, Y. and GEIGER, J., "Impact of nonlinear 3D equilibrium response on edge topology and divertor heat load in Wendelstein 7-X", Plasma Phys. Control. Fusion **58** (2016) 064004